IOPscience iopscience.iop.org

Home Search Collections Journals About Contact us My IOPscience

The absolute efficiency of resonant Raman scattering by longitudinal optical phonons in ZnTe near the E_0 gap

This article has been downloaded from IOPscience. Please scroll down to see the full text article.

1994 J. Phys.: Condens. Matter 6 6057

(http://iopscience.iop.org/0953-8984/6/30/023)

View the table of contents for this issue, or go to the journal homepage for more

Download details:
IP Address: 171.66.16.147
The article was downloaded on 12/05/2010 at 19:03

Please note that terms and conditions apply.

J. Phys.: Condens. Matter 6 (1994) 6057–6065. Printed in the UK

The absolute efficiency of resonant Raman scattering by longitudinal optical phonons in ZnTe near the E_0 gap

H Leiderer†, M Silberbauer†, S Bauer†, W Limmer‡ and W Gebhardt†

† Institut für Festkörperphysik, Universität Regensburg, D-93053 Regensburg, Universitätsstraße 31, Germany

‡ Abteilung Halbleiterphysik, Universität Ulm, D-89069 Ulm, Germany

Received 11 February 1994, in final form 3 May 1994

Abstract. The absolute efficiency of resonant Raman scattering by longitudinal optical phonons is determined for an orientated ZnTe bulk crystal and single-crystalline ZnTe epilayers with incident photon energies near the E_0 band gap at a temperature of 2 K. The ZnTe layers were grown by metal–organic vapour-phase epitaxy (MOVPE) on (001) GaAs and (001) GaSb, respectively, with a thickness of about 2 μm. Absolute values of the Raman scattering efficiency (RSE) have been determined in $z(x,x)\bar{z}$ and $z(y,x)\bar{z}$ backscattering configuration using a sample-substitution method and correcting the measured intensities with respect to absorption, reflection, and refraction. Measurements of the absorption coefficient and the reflectivity were performed on the same samples and at the same temperature. Well resolved maxima of the RSE appear at the $m = 1$ and $m = 2$ discrete energy levels of the band-gap exciton for incoming resonance and at the $m = 1$ level for outgoing resonance. Valence-band splitting due to residual biaxial strain in the ZnTe epilayers results in a splitting of the $m = 1$ resonance maximum for both incoming and outgoing resonance.

1. Introduction

In semiconductors the Raman scattering efficiency (RSE) by optical phonons exhibits a resonant enhancement whenever the energy of the incident (incoming resonance) or scattered light (outgoing resonance) approaches a critical point in the density of electronic excitations [1, 2]. This phenomenon, known as resonant Raman scattering (RRS), has been investigated experimentally and theoretically in a large number of III–V and II–VI semiconductors.

Raman scattering by one longitudinal optical (LO) phonon is usually described in time-dependent perturbation theory as a three-step process where a part of the photon energy is transferred to the phonon system via intermediate electronic states. A quantitative comparison between theoretical and experimental results has shown that the discrete and continuous states of Wannier–Mott excitons have to be considered as intermediate electronic states for scattering near the E_0 and $E_0 + \Delta_0$ gap [3–10].

Experimental resonance profiles of the RSE, frequently recorded at liquid-nitrogen temperature, normally exhibit one maximum for incoming and one maximum for outgoing resonance found at the energetic position of the $m = 1$ exciton ground state. Absolute values of the RSE are usually determined using a sample-substitution method and correcting the measured intensities with respect to the optical constants [1, 2]. However, in most cases values for the optical constants are taken from literature and have to be modified in order to fit the experimental conditions. In this paper absolute values for the RSE of a ZnTe bulk

0953-8984/94/306057+09$19.50 © 1994 IOP Publishing Ltd

crystal and ZnTe epilayers are presented where measurements of the absorption coefficient and the reflectivity were performed on the same samples and at the same temperature. The measurements were carried out at a temperature of $T = 2$ K in order to resolve resonance structures of the RSE due to discrete exciton levels with $m > 1$.

2. Raman scattering efficiency

Scattered Raman intensities are usually expressed by the RSE $\mathrm{d}S/\mathrm{d}\Omega$. This quantity has the dimension of an inverse length and represents the ratio between scattered and incident power for a unit solid angle and a unit path length within the crystal. It is defined as

$$\frac{\mathrm{d}S}{\mathrm{d}\Omega} = \frac{\mathrm{d}P_S}{\mathrm{d}\Omega}\frac{1}{P_L L} \tag{1}$$

where $\mathrm{d}P_S/\mathrm{d}\Omega$ denotes the scattered power per solid angle $\mathrm{d}\Omega$ inside the crystal, P_L is the incident power, and L is the scattering length. For Stokes scattering by one LO phonon it can be written in terms of the corresponding Raman tensor $\mathbf{R}$ [10]:

$$\frac{\mathrm{d}S}{\mathrm{d}\Omega} = \frac{\omega_S^3\omega_L}{c^4}\frac{\hbar^2}{2v_c M^*\hbar\Omega_{\mathrm{LO}}}\frac{n_S}{n_L}(\bar{n}+1)|\,e_S^*\cdot\mathbf{R}\cdot e_L\,|^2 \tag{2}$$

where ω is the photon frequency, $\bar{n}$ the phonon occupation number, e the photon polarization vector, and n the index of refraction. The quantities referring to the incident and scattered photons have subscripts L and S, respectively. Ω_{LO} is the LO-phonon frequency, c the speed of light in vacuum, v_c the volume of the primitive cell and M^* its reduced mass. For backscattering at the (001) surface of zincblende-type crystals the Raman tensors for scattering via deformation-potential (DP) and Fröhlich (F) interaction are given by

$$\mathbf{R}_{\mathrm{DP}} = \begin{pmatrix} 0 & a_{\mathrm{DP}} & 0 \\ a_{\mathrm{DP}} & 0 & 0 \\ 0 & 0 & 0 \end{pmatrix} \qquad \mathbf{R}_{\mathrm{F}} = \begin{pmatrix} a_{\mathrm{F}} & 0 & 0 \\ 0 & a_{\mathrm{F}} & 0 \\ 0 & 0 & a_{\mathrm{F}} \end{pmatrix}. \tag{3}$$

Analytical expressions for the resonant Raman polarizabilities a_{DP} and a_{F} including the discrete and continuous states of Wannier–Mott excitons as intermediate electronic states are given in [6, 10]. According to equations (2) and (3) scattering via deformation-potential and Fröhlich interaction is observed in $z(y,x)\bar{z}$ and $z(x,x)\bar{z}$ scattering configuration, respectively.

3. Experimental details

ZnTe layers with thicknesses of about 2 μm were grown on (001) GaAs and (001) GaSb at an optimized growth temperature of 350 °C using diethylzinc and diisopropyltelluride in an atmospheric-pressure MOVPE system [11]. The ZnTe epilayers exhibit in-plane strain fields on both substrates used. The strain is produced by lattice mismatch and by different thermal expansion of substrate and layer. In the case of ZnTe/GaAs we obtain a lattice mismatch of –7.48% at growth temperature. The mismatch is –0.22% for the heterostructure ZnTe/GaSb. The corresponding compressive strain is reduced by the generation of misfit dislocations at a critical thickness [12, 13]. However, there is still residual strain after this partial relaxation which reduces the T_d symmetry of ZnTe to D_{2d}. For a zincblende-type semiconductor such as ZnTe the valence band edge at $k = 0$ consists of a fourfold Γ_8 multiplet ($J = \frac{3}{2}; m_j = \pm\frac{3}{2}, m_j = \pm\frac{1}{2}$). The application of biaxial stress splits the Γ_8 multiplet, because of the reduced symmetry. The substates of the Γ_8 valence band are

labelled HH ($J = \frac{3}{2}; m_j = \pm\frac{3}{2}$) and LH ($J = \frac{3}{2}; m_j = \pm\frac{1}{2}$) in this paper. The corresponding excitons are called HH and LH excitons.

For the Raman measurements a CW dye laser operating with Coumarin 510 and pumped by the 458 nm line of an Ar^+-ion laser was used as a tunable excitation source in the spectral range 2.15–2.45 eV. All measurements were performed in backscattering configuration with the direction of incident and scattered light perpendicular to the (001) surface of the ZnTe samples or the ZnSe standard. We denote the [100], [010], and [001] directions of the crystals by x, y and z, respectively. The surfaces of the epilayers are as grown and the bulk crystal was polished on a microcloth saturated with a suspension of 0.05μm alumina powder in distilled water.

Absolute values of the RSE were obtained by using a sample-substitution method [1] with the 258 cm^{-1} one-LO-phonon line of ZnSe as a reference [14]. The measured integrated scattering rates R of sample and $\tilde{R}$ of reference outside the crystal are related to the RSE by [1, 2]

$$\frac{dS}{d\Omega} = \frac{\tilde{K}}{K}\frac{d\tilde{S}}{d\Omega}\frac{R}{\tilde{R}} \tag{4}$$

with

$$K = \frac{(1-r_L)(1-r_S)\{1-\exp[-(\alpha_L+\alpha_S)L]\}}{n_S^2(\alpha_L+\alpha_S)}. \tag{5}$$

The frequency-dependent factors K and $\tilde{K}$ must be used to correct R and $\tilde{R}$ with respect to absorption (α), reflectivity (r) and refraction (n) for incident and scattered light.

The optical constants of the ZnTe samples and the ZnSe standard were obtained from transmission and reflectivity measurements carried out in our laboratory [15–17] at the same temperature of 2 K. For this purpose a halogen lamp was used as a light source for the normal-incidence experiments.

The split exciton structure due to residual strain in the layers is determined from reflectivity spectra in comparison with a model from Hopfield and Thomas [18]. The transverse HH- and LH-exciton energies E_T can be determined in this way [17].

For the transmission measurements the epitaxial layers were glued on a small glass plate and the substrate was removed by mechanical polishing and chemical etching. The ZnTe samples were washed in acetone in order to remove the glue and were mounted as free-standing layers in a special bag to avoid movement during the experiment at 2 K. The thickness of the samples was measured with Fabry–Perot interferences in the transparent region. The absorption coefficient near the E_0 band gap is governed by the well separated contributions from the HH and LH excitons and is well fitted by an analytical expression given by Goñi *et al* [19]. From the fit we derived the absolute absorption amplitudes, exciton energies and phenomenological damping constants for the discrete and continuous exciton states. However, the positions of the exciton energies are changed in the transmission spectra in relation to the reflectivity measurements. The strain in the epilayer changed with the preparation of a free-standing layer. In order to obtain the absorption coefficient of the original heterostructure we shifted the position of the exciton absorption in our transmission spectra to the values observed in reflectivity.

The absorption coefficient of the semi-infinite bulk sample was not directly measured, because it is difficult to prepare a transparent layer in the exciton region from a bulk crystal. Therefore, we used the absorption coefficient of the epitaxial layers corrected for the degenerate exciton structure in the bulk sample which was measured by reflectivity (figure 2(a)).

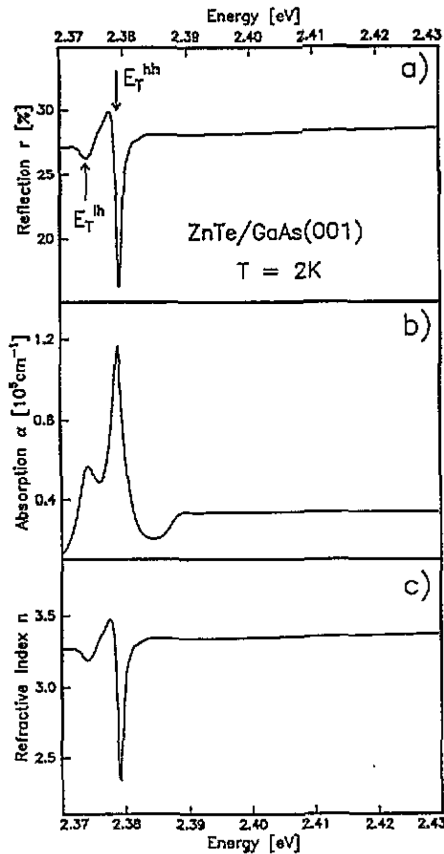

Figure 1. Optical constants of the 2 μm thick ZnTe epilayer on (001) GaAs at a temperature of 2 K. They are used to correct the measured Raman scattering rates with respect to reflectivity (a), absorption (b) and refractive index (c) in equation (5).

The refractive index can be calculated with knowledge of the reflectivity r and the absorption coefficient α. The relation is given by

$$n = \frac{(r+1) + \left[4r - (r-1)^2\alpha^2\lambda^2/16\pi^2\right]^{1/2}}{(1-r)} \tag{6}$$

where λ denotes the wavelength of the light.

Figure 1 shows as an example the optical constants of the ZnTe epilayer on GaAs at a temperature of 2 K obtained in the way described. For reflectivity, absorption coefficient and refractive index HH well resolved structures due to the contributions from the LH- and HH-exciton ground state ($m = 1$) are observed. The energies of the transverse LH and HH excitons are E_T(LH) = 2.374 eV and $E_T(HH) = 2.379$ eV, respectively.

4. Results

In the upper part of figures 2–4 the measured reflectivity spectra near the fundamental band gap E_0 at $T = 2$ K are shown. The dashed lines mark the energetic position E_T(LH) and E_T(HH) of the $m = 1$ transverse LH- and HH-exciton ground state, respectively. The strain-

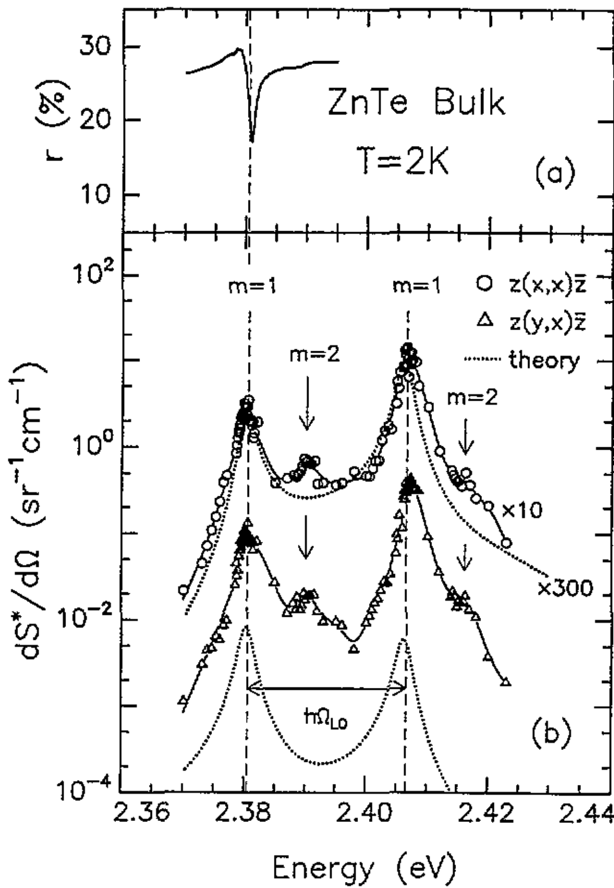

Figure 2. Reflectivity (a) and absolute RSE (b) of bulk ZnTe at $T = 2$ K. For both incoming and outgoing resonance, well resolved maxima of the RSE occur at energies of the $m = 1$ and $m = 2$ discrete exciton states. The dotted lines are calculated resonance curves assuming an electron–phonon interaction via the Fröhlich mechanism (upper curve) and via the deformation-potential mechanism (lower curve).

induced splitting of the exciton ground state amounts to 5 meV for the ZnTe/GaAs epilayer and 4 meV for the ZnTe/GaSb epilayer. Comparing the excitonic reflectivity of ZnTe/GaAs with that of ZnTe/GaSb the latter is much less broadened, indicating a higher quality of the ZnTe/GaSb sample, a result which is confirmed by photoluminescence measurements [11] and TEM experiments [12, 13].

In the lower part of figures 2–4 the absolute RSEs of the ZnTe bulk crystal and the ZnTe epilayers are displayed for the scattering configurations $z(x,x)\bar{z}$ and $z(y,x)\bar{z}$. The results for the $z(x,x)\bar{z}$ configuration are multiplied by a factor of 10 for clarity. Instead of $\mathrm{d}S/\mathrm{d}\Omega$ the quantity

$$\frac{\mathrm{d}S^*}{\mathrm{d}\Omega} = \frac{\mathrm{d}S}{\mathrm{d}\Omega}\frac{n_L}{n_S} \tag{7}$$

is plotted since in theoretical calculations of the RSE the energy dependence of n_S and n_L is usually neglected and the approximation $n_S/n_L \simeq 1$ is made in equation (2) [6, 10]. This may facilitate a detailed comparison with theoretical calculations in future publications.

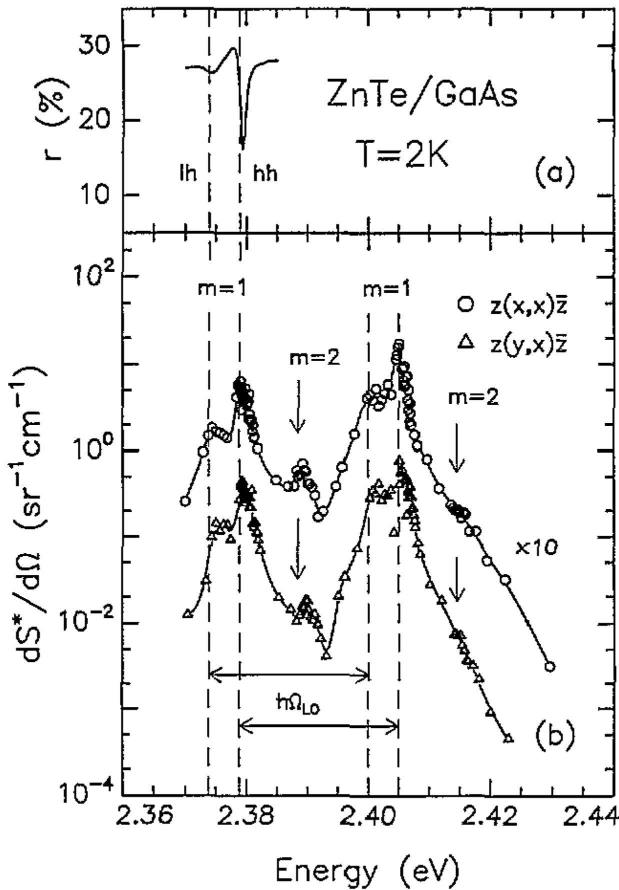

Figure 3. Reflectivity (a) and absolute RSE (b) of the ZnTe/GaAs epilayer. The strain-induced separation (5 meV) of the LH- and HH-exciton ground-state energy ($m = 1$) observed in the reflectivity spectrum is well reproduced by the RSE for both incoming and outgoing resonance. For incoming resonance even the $m = 2$ HH-exciton level is clearly resolved.

For all samples under investigation the incoming resonance of the RSE occurs exactly at $E_T = E_0 - R_y$ with the exciton Rydberg energy $R_y = 12.8$ meV and the outgoing resonance occurs at $E_T + \hbar\Omega_{LO}$ with $\hbar\Omega_{LO} = 26$ meV. This is still true when the degeneracy of the LH- and HH-exciton states is lifted. The strain-induced splitting of the exciton ground state in the ZnTe epilayers measured via reflectivity is clearly reproduced by the RSE in both incoming and outgoing resonance. Similar to reflectivity the RSE exhibits a much stronger resonance structure at the HH-exciton ground state than at the LH-exciton ground state which results from the different oscillator strengths of the two excitons. The increasing crystal quality from bulk ZnTe to ZnTe/GaAs and ZnTe/GaSb is also reflected by the RSE. In the case of ZnTe/GaSb the absolute value of the RSE at incoming resonance is about six times higher than that of the ZnTe bulk crystal and the resonance structure is much more pronounced.

For incoming resonance a further distinct maximum appears at the $m = 2$ discrete HH-exciton level with energy $E_0 - \frac{1}{4}R_y$. For outgoing resonance only a slight hump on the decreasing slope at $E_0 - \frac{1}{4}R_y + \hbar\Omega_{LO}$ is observable which is most pronounced in the bulk crystal.

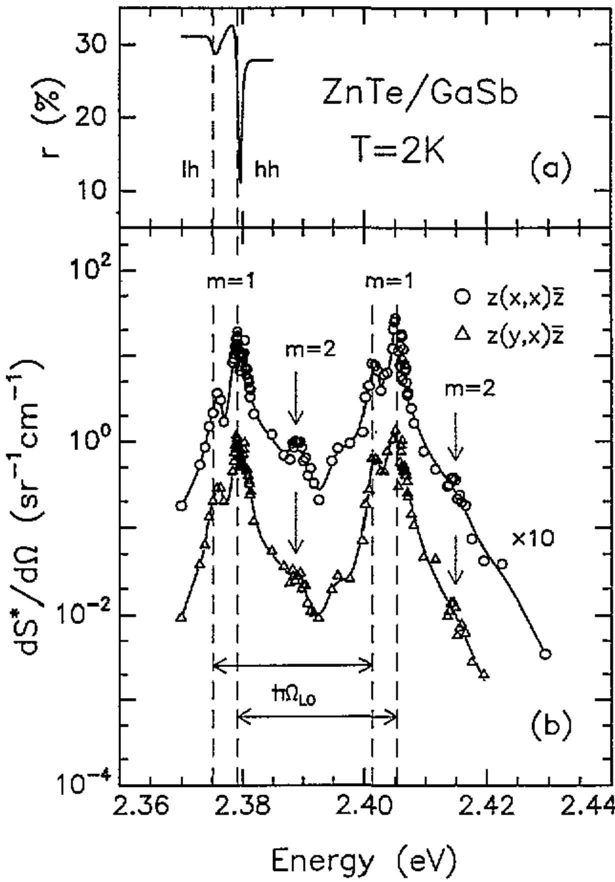

Figure 4. Reflectivity (a) and absolute RSE (b) of the ZnTe/GaSb epilayer. The resonance behaviour of the RSE is similar to that of the ZnTe/GaAs epilayer. However, the resonance maxima are more pronounced because of the better crystal quality of the ZnTe layer.

The dotted lines in figure 2(b) represent calculated resonance curves of the RSE for degenerate HH- and LH-exciton states where electron–phonon interaction via the Fröhlich mechanism (upper curve) and via the deformation-potential mechanism (lower curve) has been assumed. For the calculations we used equations (2), (3) and theoretical expressions of the Raman polarizabilities from [6, 10] where an empirical relation is given for the broadenings Γ_m of the discrete exciton states:

$$\Gamma_m = \Gamma_c - (\Gamma_c - \Gamma_1)/m^2 \qquad (m = 1, 2, 3, ...) . \tag{8}$$

The broadening parameters Γ_1 and Γ_c of the $m = 1$ discrete exciton state and the continuous exciton states were chosen as 1.3 meV and 20 meV, respectively. All other fit parameters were taken from [20]. The resonance curve of the Fröhlich interaction had to be multiplied by a factor of 30 in order to fit the experimental data near resonance. In contrast to the experimental results the calculated RSE exhibits no resonance structure at the energetic position of the discrete exciton level $m = 2$. This may be due, in part, to the special choice of broadening parameters according to the relation given in equation (8). In the case of deformation-potential interaction the calculated RSE exhibits its highest resonance maximum at $E_T = E_0 - R_y$ (incoming resonance), while the measured RSE reaches it at $E_T + \hbar\Omega_{LO}$

(outgoing resonance). Furthermore, at the resonance maxima the experimental values are about two orders of magnitude larger than the calculated ones. This phenomenon has already been observed in other II–VI semiconductors like $Zn_{1-x}Mn_xSe$ [7], $Cd_{0.8}Mn_{0.2}Te$ [10] and ZnTe ($T = 80$ K) [20]. It has been explained by a depolarization of the scattered light near resonance. This means that near resonance the Raman signal of the deformation-potential-induced scattering is superimposed by depolarized parts of scattered light which arises from the Fröhlich interaction.

In all measured resonance curves, with the exception of the $z(x,x)\bar{z}$ curve in figure 2(b), a pronounced local minimum of the RSE is clearly apparent between incoming and outgoing resonance at the energy E_0. It also appears in the uncorrected normalized scattering rates and cannot be attributed to some artefact of the correction due to the energy dependence of the absorption coefficient. The origin of this minimum is not clear, especially since it is not reproduced by the calculated curves in figure 2(b). The same applies to a slight shoulder which appears about 10 meV below the $m = 1$ HH outgoing resonance in figure 4.

The experimentally observed structures in the resonance behaviour, not reproduced by our calculations of the RSE in bulk ZnTe, may be the topic of further detailed theoretical studies, where the strain-induced splitting of the HH and LH valence bands in the ZnTe epilayers should also be taken into account.

5. Conclusion

We have determined the absolute Raman scattering efficiency of a ZnTe bulk crystal and two ZnTe epilayers at $T = 2$ K for incident photon energies near the E_0 band gap. The ZnTe layers were grown by MOVPE on (001) GaAs and (001) GaSb, respectively, with a thickness of about 2 μm. The absolute RSE measured in $z(x,x)\bar{z}$ and $z(y,x)\bar{z}$ backscattering configuration was determined by using a sample-substitution method and correcting the measured intensities with respect to absorption, reflection and refraction. In the case of the ZnTe/GaAs and ZnTe/GaSb epilayers both incoming and outgoing resonance of the RSE exhibit a double structure which is explained by the strain-induced splitting of the exciton ground state. In all samples a clearly resolvable maximum of the RSE at the $m = 2$ HH-exciton level is observed for incoming resonance.

Acknowledgments

We would like to thank W Kuhn and H P Wagner for kindly providing us with the ZnTe epilayers as well as W Prettl for the ZnTe bulk crystal. This work was supported by the Deutsche Forschungsgemeinschaft (DFG) and the Bundesministerium für Forschung und Technologie (BMFT).

References

[1] Cardona M 1982 *Springer Topics in Applied Physics* vol 50, ed M Cardona and G Güntherodt (Berlin: Springer)
[2] Richter W 1976 *Springer Tracts in Modern Physics* vol 78, ed G Höhler (Berlin: Springer)
[3] Cantarero A, Trallero-Giner C and Cardona M 1989 *Phys. Rev.* B 39 8388
[4] Trallero-Giner C, Gavrilenko V I and Cardona M 1989 *Phys. Rev.* B **40** 1238
[5] Trallero-Giner C, Cantarero A and Cardona M 1989 *Phys. Rev.* B 40 4030
[6] Cantarero A, Trallero-Giner C and Cardona M 1989 *Phys. Rev.* B **40** 12 290
[7] Limmer W, Leiderer H, Jakob K, Gebhardt W, Kauschke W, Cantarero A and Trallero-Giner C 1990 *Phys. Rev.* B **42** 11 325

[8] Gavrilenko V I, Trallero-Giner C, Cantarero A and Cardona M 1990 *Phys. Rev.* B **42** 11 875
[9] Trallero-Giner C, Cantarero A, Cardona M and Mora M 1992 *Phys. Rev.* B **45** 6601
[10] Limmer W, Bauer S, Leiderer H, Gebhardt W, Cantarero A, Trallero-Giner C and Cardona M 1992 *Phys. Rev.* B **45** 11 709
[11] Wagner H P, Kuhn W and Gebhardt W 1990 *J. Cryst. Growth* **101** 199
[12] Bauer S, Rosenauer A, Skorsetz J, Kuhn W, Wagner H P, Zweck J and Gebhardt W 1992 *J. Cryst. Growth* **117** 297
[13] Bauer S, Rosenauer A, Kuhn W, Link P, Zweck J and Gebhardt W 1993 *Ultramicroscopy* **51** 221
[14] Calleja J M, Vogt H and Cardona M 1982 *Phil. Mag.* A **45** 239
[15] Langen B, Leiderer H, Limmer W, Gebhardt W, Ruff M and Rössler U 1990 *J. Cryst. Growth* **101** 718
[16] Leiderer H, Supritz A, Silberbauer M, Lindner M, Kuhn W, Wagner H P and Gebhardt W 1991 *Semicond. Sci. Technol.* A **6** 101
[17] Leiderer H, Jahn G, Silberbauer M, Kuhn W, Wagner H P, Limmer W and Gebhardt W 1991 *J. Appl. Phys.* **70** 398
[18] Hopfield J J and Thomas D G 1963 *Phys. Rev.* **132** 563
[19] Goñi A R, Cantarero A, Syassen K and Cardona M 1990 *Phys. Rev.* B **41** 10 111
[20] Limmer W, Leiderer H, Jakob K and Gebhardt W 1990 *Proc. 20th Int. Conf. on the Physics of Semiconductors (Thessaloniki, 1990)* ed E M Anastassakis and J D Joannopoulos (Singapore: World Scientific) p 2005